

# Scaling the response of circular plates subjected to large and close-range spherical explosions. Part II: Buried charges

A. Neuberger<sup>a,b,\*</sup>, S. Peles<sup>c</sup>, D. Rittel<sup>a</sup>

<sup>a</sup>*Technion, Faculty of Mechanical Engineering, Israel Institute of Technology, 32000 Haifa, Israel*

<sup>b</sup>*MOD, Tank Program Management, Hakiryia, Tel-Aviv, Israel*

<sup>c</sup>*IMI, Central Laboratory Division, Ramat Hasharon, P.O. Box 1044, Israel*

Received 5 January 2006; accepted 9 April 2006

Available online 12 June 2006

---

## Abstract

This paper discusses scaling of the dynamic response of clamped circular plates subjected to close-range, large spherical blast loadings that are flush buried in dry sand. As a continuation of part I which dealt with air blasts, similarity is obtained by using replica scaling for all geometrical parameters, while the blast effect is scaled by using the Hopkinson scaling law.

In the case of buried charges, both the depth of burial and nature of the soil have a significant effect on the energy which is directed towards the target by funneling and magnifying it upwards. This paper addresses the effect of flush burial on the target's dynamic response compared to a target loaded by similar air-blast energy.

We present numerical and experimental results from a series of controlled explosion experiments. The experimental and numerical results agree quite well, so that the main outcome of this study is that scaling can be successfully applied to assess the dynamic response of circular steel armor plates subjected to close-range, buried large spherical explosions.

© 2006 Elsevier Ltd. All rights reserved.

*Keywords:* Close-range; Dynamic response; Circular plate; Scaling; Buried charge

---

## 1. Introduction

Developing efficient protection systems against large buried charges of high explosive requires numerical and experimental work. In the case of full-scale development field experiments, the preparations and measurements are complex and expensive. Experiments at reduced scale can identify critical effects, improve engineering design, and validate physics-based models that can be used to predict the structural dynamic response at all scales.

As mentioned in part I of this paper, the currently available hydrodynamic computer codes can produce detailed and instructive pictures of the charges' effects as a function of time. However, for the problem of buried charges, the finite element calculations are more complicated and require combined Lagrangian mesh for the solid structure and Eulerian mesh for the high explosive charge, air and surrounding soil.

---

\*Corresponding author. MOD, MANTAK, Tank Program Management, 3200 Hakiryia, Tel-Aviv, Israel.

E-mail address: [navidov@gmail.com](mailto:navidov@gmail.com) (A. Neuberger).

### Nomenclature

$a$	generalized Mohr–Coulomb model coefficient
$b$	generalized Mohr–Coulomb model coefficient
$D$	plate diameter
$P$	pressure
$R^*$	distance from center of spherical charge
$S$	scaling factor
$s_{ij}$	components of the deviatoric stress tensor
$t$	plate thickness
$W$	charge weight
$Y_{\max}$	upper limit of soil's strength
$\delta$	peak deflection
$\varepsilon, \dot{\varepsilon}$	strain, strain rate
$\sigma$	stress
$\tau$	time

Laine et al. [1] performed numerical simulations and reported a significant effect of different kinds of mine burial and soil materials on the dynamic loading. For buried mines, it was found that the incident maximum pressure and impulse straight above the mine are significantly influenced by the nature and properties of the soil material. Williams et al. [2] presented a parametric study using two empirical loading models, ConWep and the mine loading model developed by Westine et al. [3], to predict the effect of a 6 kg mine blast on a simple structure. The main outcome of this work was that the simplified blast models are limited, so that in order to accurately represent the ground conditions, these models must be scaled and calibrated against experimental results.

When a high explosive charge is detonated in soil, the depth of burial and the type of soil have a significant effect on the energy, which is directed to the target by funneling or reflecting it upwards. To the best of the authors' knowledge, studies on the scaling of buried charges effects were not reported. Furthermore, the combination of *scaling* the dynamic response of an armor steel plate subjected to a very *large explosion* from a *close range buried charge* was not studied yet.

Therefore, this paper presents a scaling procedure for clamped circular plates subjected to large buried spherical charges. Similar to part I, scaling is obtained by using replica scaling for all geometrical parameters, while the blast effect is scaled by using Hopkinson's scaling law. Whereas it is common knowledge that the shape of the charge has its own influence, a spherical TNT charge, initiated from its center, is used throughout this study as a generic problem. The surrounding soil is chosen as dry sea sand, and the charge is buried right underneath the soil's surface (flush burial). The effects of buried and air-detonated charges are presented and compared. This comparison can be applied to approximate the buried charge effects by a simplified air blast model.

The paper is organized as follows: Section 2 presents the numerical approach, followed by Section 3 that describes the test setup and measuring technique. Section 4 presents the numerical results, followed by the experimental results. Section 5 discusses the key points of the study, followed by concluding remarks.

## 2. Numerical simulations

A detailed description of the numerical method has been given in the first part of the paper. We will therefore briefly remind the main procedures and emphasize only points that are relevant to the buried charge problem. The numerical simulations were carried out using LS-DYNA finite element code [4]. The simulation of the dynamic structural response was carried out using the coupled Lagrangian–Eulerian method. The multi-material Eulerian formulation is part of the Arbitrary-Lagrangian–Eulerian (ALE) solver within LS-DYNA.

One approach consists of combining the ALE solver with an Eulerian–Lagrangian coupling algorithm, in which a structural or Lagrangian mesh can interact with the gas products propagating in the soil/air (represented by an Eulerian mesh), as shown in Fig. 1. One should note that this technique is quite time consuming. An alternative approximate approach combines a pure Lagrangian method with a simplified engineering blast model, such as ConWep [5]. However, this can only be done after calibration of the buried charge effect with respect to standard air blast effect. The two approaches were used throughout this work.

In part I, the numerical calculations chapter comprised 4 distinct stages. The following results related to flush buried charges can be viewed as the fifth stage that completes the study. Part I addressed the effect of variations of mechanical properties with plate thickness on its response. The present simulations include these variations, according to Table 1 of part I. The material properties are divided into three sets of plate thickness, and the present calculations were carried out for one representative element of each set. Consequently, three different scale factors were simulated, namely  $S = 1, 2, \text{ and } 4$ .

Therefore, the problem at hand is similar to that discussed in detail in part I, with the exception that the charge is now *flush buried in dry sand*. The following parameters were selected: plate thickness  $t = 0.04 \text{ m}$ , plate diameter  $D = 2 \text{ m}$ , charge's weight  $W = 50 \text{ kg}$  TNT (flush buried in dry sand), and the distance from the plate's surface to the center of the charge  $R = 0.5 \text{ m}$ . The steel plate was modeled using Johnson–Cook model [6] as mentioned in part I.

### 2.1. Material behavior

The steel armor material, air and charge properties are identical to those detailed in part I regarding the ALE calculations. One additional material is the soil that surrounds the charge. Its main effect is to cause upward reflection of the blast wave.

The constitutive behavior of geomaterials differs from that of metals in three important ways: geomaterials are compressible, i.e. pressure–volume response; the yield strength of geomaterials depends on the mean stress (pressure), i.e. frictional response; finally, the tensile strength of geomaterials is negligible compared to their compressive strength.

Soil properties appear to vary considerably depending upon the location, type, moisture content, porosity, aggregate size, ambient temperature and humidity conditions. This variability can significantly affect the interacting loading mechanisms and generate different load functions.

The simplest constitutive model used for a dry soil is the generalized Mohr–Coulomb model [7,8]

$$Y = a + b \cdot P, \quad (1)$$

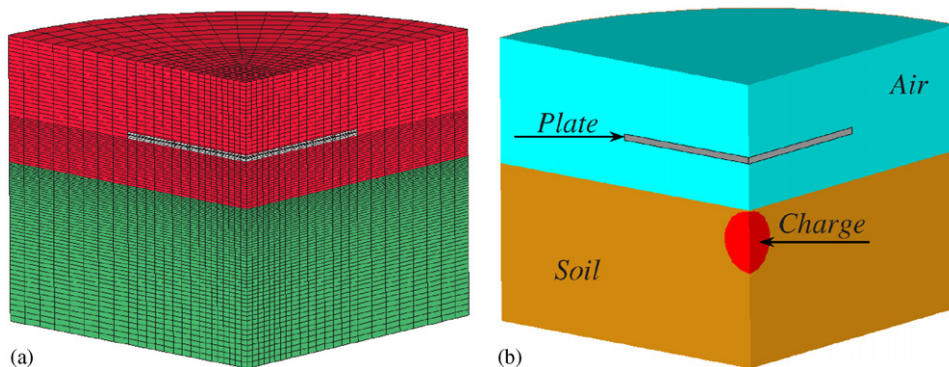


Fig. 1. Finite elements model: (a) Eulerian (soil, air, charge) and Lagrangian (plate) mesh; (b) initial volume fraction of the components of the model.

where

$$Y = \sqrt{3J_2} = \sqrt{\frac{3}{2}s_{ij}s_{ij}} \quad \text{and} \quad P = \frac{1}{3}J_1 = \frac{1}{3}(\sigma_1 + \sigma_2 + \sigma_3), \quad (2)$$

where  $s_{ij}$  are the components of the deviatoric stress tensor, and  $P$  is the hydrostatic pressure.

The coefficients  $a$  and  $b$  can be evaluated from the soil material constants known as the cohesion strength and the angle of friction. An improvement of this simple model is needed for situations involving very large pressures to provide an upper bound for strength as the pressure increases noticeably. Consequently, we included a third parameter,  $Y_{\max}$ , to limit the soil strength, so that the final constitutive soil model becomes

$$Y = \min(a + b \cdot P, Y_{\max}). \quad (3)$$

In this work, the soil parameters were:  $Y_{\max} = 4.8$  MPa,  $a = 0$  MPa, and  $b = 1.46$ .

### 3. Test setup

Two different scaled-down similar test rigs ( $S = 2$  and  $4$ ) were built in order to experimentally assess the applicability of scale-down modeling of the studied problem. The experimental test setup of each structure is shown in Fig. 2. The target plate was supported by two thick armor steel plates with circular holes that were tightened together with bolts and clamps. The thick plate that faces the charge has a hole with inclined side walls to prevent reflection of the blast wave to the tested plate. To consistently use the same sand conditions, a sturdy steel container was built and filled with dry sand for each explosion. The spherical TNT charges were flush buried in the dry sand as shown schematically in Fig. 3.

The measurement of the maximum dynamic deflection of the plate was achieved, as previously, by means of a specially devised comb-like device.

## 4. Results

### 4.1. Numerical results

Fig. 4 shows a typical result of the ALE calculation showing the interaction between the explosive gas products and the steel plate. The explosive products are clearly funneled towards the plate. Fig. 5 shows the evolution of the normalized maximum deflection at three different scales. This figure can be compared with Figure 10 (part I) to assess the amplification effect of the charge burial, which leads to a much larger deflection of the plate. In this simulation, the variability of material properties with plate thickness has been accounted for, so that the midpoint deflections do not strictly overlap at the various scales (see part I). Fig. 6 shows the evolution of the effective stress for the same problem. By comparing with Figure 11 of part I, it can be noted



Fig. 2. Experimental setup at 2 different scales ( $S = 4$ , left and  $S = 2$ , right)

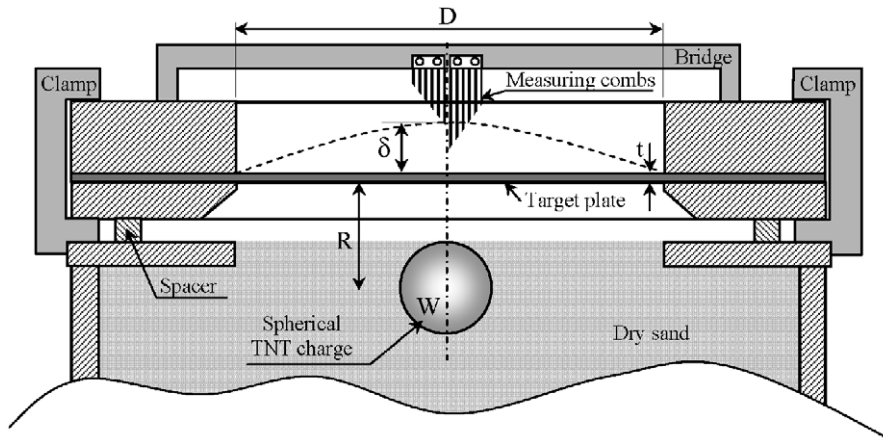


Fig. 3. Schematic drawing of the test rig and the measurement setup.

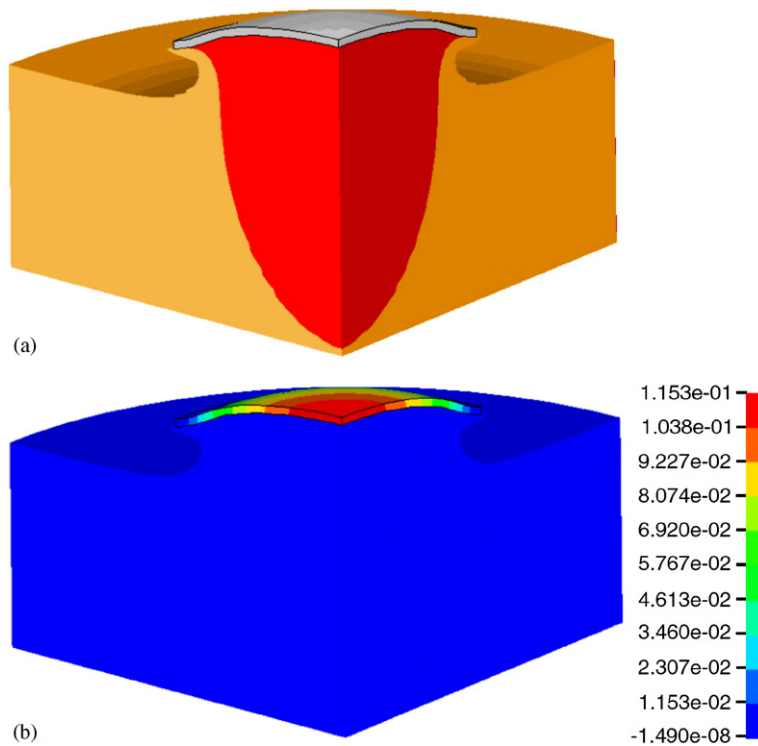


Fig. 4. (a) The soil and detonation products shape at time  $t = 1$  ms after the explosion; (b) The vertical displacement (m) of the circular plate at the same time.

that, whereas the maximum stress values remain the same, the duration of the initial peak phase is significantly larger (about twice) when the charge is flush buried.

#### 4.2. Experimental results

Two different scaled charges ( $W = 30/S^3$  and  $W = 50/S^3$  kg TNT, where  $S = 2$  and  $4$ ) were flush buried and detonated from different distances from the tested plates. The experimental results are summarized in Figs. 7

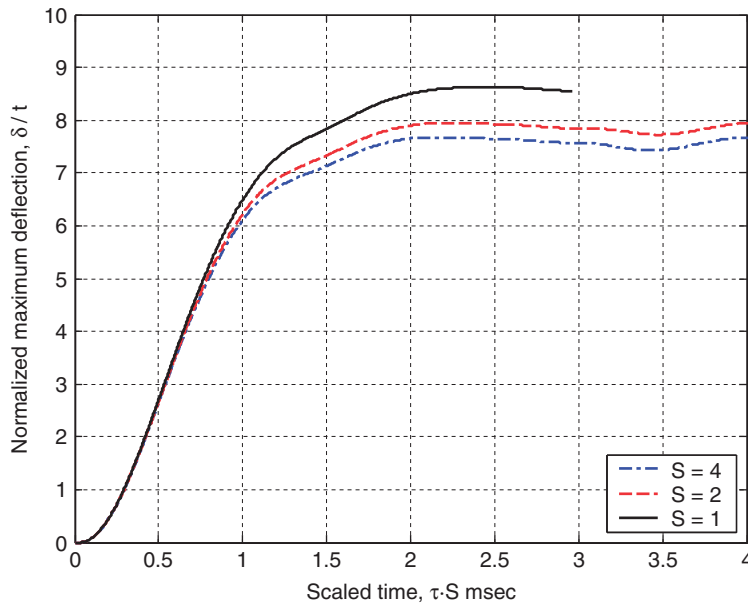


Fig. 5. Normalized deflection at different scales vs. scaled time (material properties vary with thickness) for  $W = 50$  kg TNT flush buried in dry sand,  $R = 0.5$  m,  $D = 2$  m,  $t = 0.05$  m.

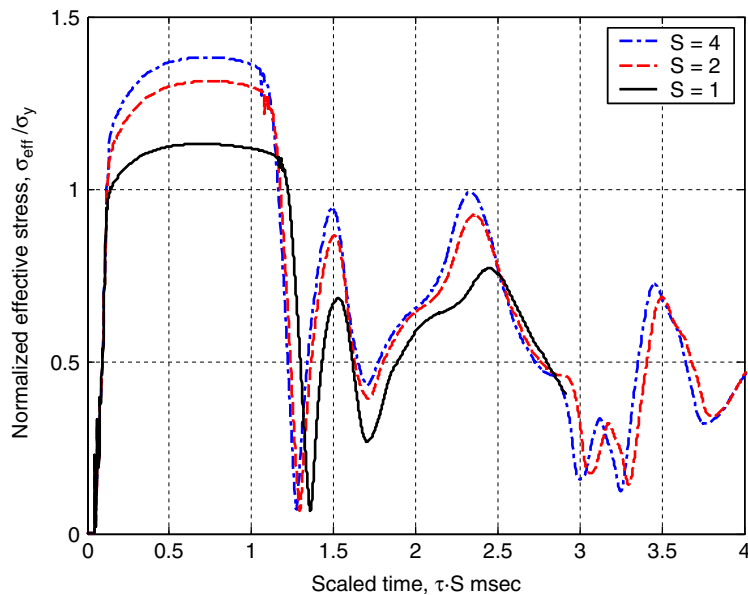


Fig. 6. Normalized effective stress at different scales vs. scaled time (material properties vary with thickness) for  $W = 50$  kg TNT flush buried in dry sand,  $R = 0.5$  m,  $D = 2$  m,  $t = 0.05$  m.

and 8 that show the maximum measured normalized deflection vs. the scaled distance from the charge’s center. These results are compared with the numerical calculations (lines). An overall excellent agreement can be noted between the experimental and numerical results. One should note that the numerical results were obtained after calibrating the constitutive parameters of the soil once the first experiment was performed. All the subsequent numerical calculations were performed with this fixed set of parameters, so that the comparison between experiment and calculation is meaningful since the numerical parameters were not



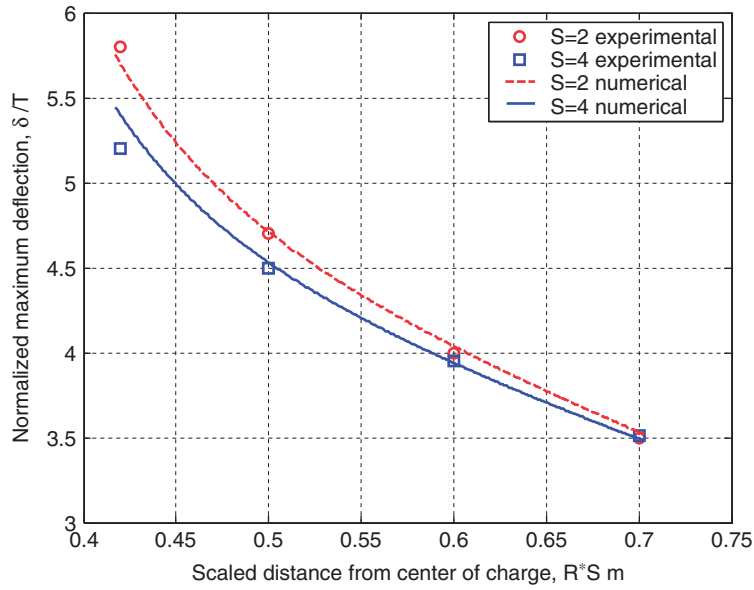


Fig. 7. Normalized maximum deflection vs. scaled distance from the center of charge for  $t \cdot S = 0.04$  m,  $t/D = 0.02$ , and  $W = 30/S^3$  kg TNT.

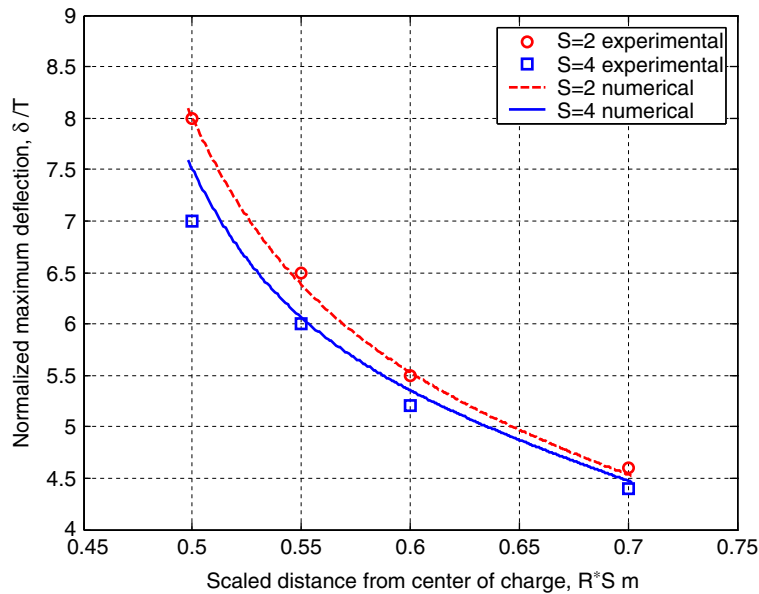


Fig. 8. Normalized maximum deflection vs. scaled distance from the center of charge for  $t \cdot S = 0.04$  m,  $t/D = 0.02$ , and  $W = 50/S^3$  kg TNT.

further adjusted. Figs. 7 and 8 also show that, as the scaled distance decreases, the agreement between the experiments and the calculations decreases slightly, and this can again be attributed to differences in mechanical (plastic) properties of the plate at different thicknesses. Yet, these figures show that the problem can be scaled for all practical purposes.

Having established the validity of the scaling concepts for the specific problem at hand, one can perform a simple scaled down test to assess the effect of the soil and burial with respect to free air detonation. These tests can be used to simulate the buried charge by a simplified blast model (e.g. ConWep) of the free-air

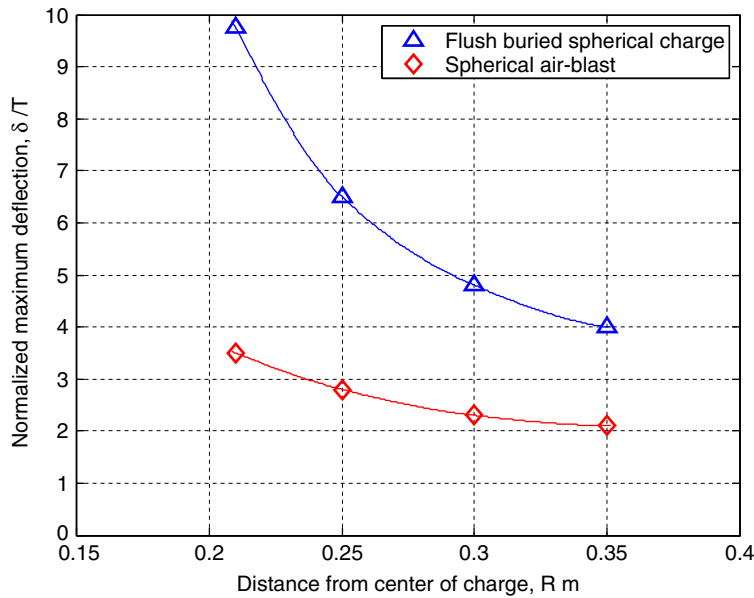


Fig. 9. A comparison of the normalized maximum deflection vs. distance from the center of charge (m) for spherical flush buried and spherical air-blast for the following scaled parameters  $t^*S = 0.04$  m,  $t/D = 0.02$ , and  $W = 40/S^3$  kg TNT.

charge. Fig. 9 shows typical results of such experiments in which the maximum normalized deflection of the plate is plotted as a function of the distance from the center of the charge, for the 2 above-mentioned cases. From Fig. 9, it appears that the magnifying ratio of the maximum normalized deflections is not constant, strictly speaking, but it decreases from 3 to 2 as the normalized distance increases from 0.21 to 0.35.

## 5. Discussion

The present work deals with flush-buried charges, as a complement to the free-air charges addresses in part I of this paper. In this case, an important preliminary step is that of the calibration of the constitutive parameters of the soil versus typical experiments. In other words, the parameters are first extracted from the literature. Then, an experiment and its simulation are performed, and the parameters are adjusted so that the simulation closely replicates the experiment. From thereon, these parameters are used for all the subsequent simulations. Once this step is successfully carried out, one can proceed to investigate the extent to which the problem of the buried charge can be calibrated using a procedure that is similar to that used for free-air charges. The numerical results show, as expected, a clear influence of the charge burial. The comparison of buried and air detonated charges shows that the former causes much larger plate deflections on the one hand, while extending the duration of the peak loading phase experienced by the plate.

The main outcome of this study appears in Figs. 7 and 8, in which it is shown that for all practical applications, the buried charge problem can indeed be scaled, as evidenced from both numerical calculations and experiments, including the very good agreement between the two.

Another important result is that, since the numerical calculations based on the ALE approach are quite time consuming, the problem can be approximated and thus simplified, by translating the buried charge problem into a free-air problem for which simplified codes such as ConWep are routinely used. In the investigated range of scaled distances between the charge center and the plate, our experimental results show that the magnifying effect of the buried charge depends on the distance from the charge as shown in Fig. 9. This dependence, once characterized, can be used to characterize the structural response at various scales of the same problem, thus simplifying considerably both the design and experimental stages.



## 6. Conclusions

A scaling procedure for the dynamic deformation of constrained steel circular plates subjected to large explosions of flush buried spherical charges has been assessed with respect to experimental results. This study indicates that the problem can be successfully scaled down, as confirmed by the comparison between experimental and numerical results.

A significant simplification of the problem can be achieved by systematically comparing the buried and the free-air charge effects, and thus using the latter to approximate the structural response to a buried charge, with the appropriate magnification factor.

The proposed parallel between these two cases can be further diversified by taking advantage of the scalability of the problem that was established in this work.

## Acknowledgements

This research was partly supported by Col. Asher Peled Memorial Research (Grant #2005650). The authors would like to thank Dr. David Touati from IMI, Central Laboratory Division, for his support and useful suggestions during the study. Useful discussions with Prof. S.R. Bodner are acknowledged.

## References

- [1] Laine L, Ranestad Ø, Sandvik A, Snekkevik A. Numerical simulation of anti-tank mine detonations. In: Proceedings of the 12th Conference of the American Physical Society, Topical Group on Shock Compression of Condensed Matter, Atlanta, USA: American Physical Society, vol. 620, 24–29 June 2001. p. 431–434.
- [2] Williams K, McClennan S, Durocher R, St-Jean B, Tremblay J. Validation of a loading model for simulating blast mine effect on armored vehicles. In: Proceedings of the 7th International LS-DYNA Users Conference, Dearborn, MI: Livermore Software Technology Corporation (LSTC), 19–21 May 2002. Session 6, p. 35–44.
- [3] Westine PS, Morris BL, Cox PA, Polch EZ. Development of computer program for floor plate response from land mine explosions. Technical Report No. 13045, US Army Tank-Automotive Command, Warren, MI, 1985.
- [4] LS-DYNA, Livermore Software Technology Corporation. Lawrence Livermore National Laboratory, Livermore, CA, USA.
- [5] ConWep, Conventional Weapons Effects, US Army TM-855, 1992.
- [6] Johnson GR, Cook WH. A constitutive model and data for metals subjected to large strain, high strain rates and high temperature. In: Proceedings of the 7th International Symposium on Ballistics, The Hague, The Netherlands, 1983. p. 541–548.
- [7] Hoek VD. Modeling of concrete by a Mohr–Coulomb model. Pisces International Technical Note TN-7802, March 1978.
- [8] Drucker DC, Prager W. Soil mechanics and plastic analysis on limit design. *Q Appl Math* 1952;10:157–65.